

Published in final edited form as:

Ultrasonics. 2014 July ; 54(5): 1162–1169. doi:10.1016/j.ultras.2013.09.025.

Multi-frequency Axial Transmission Bone Ultrasonometer

Alexey Tatarinov, Vladimir Egorov, Noun Sarvazyan, and Armen Sarvazyan

Artann Laboratories, Trenton, NJ 08618, USA

Abstract

The last decade has seen a surge in the development of axial transmission QUS (Quantitative UltraSound) technologies for the assessment of long bones using various modes of acoustic waves. The condition of cortical bones and the development of osteoporosis are determined by numerous mechanical, micro-structural, and geometrical or macro-structural bone properties like hardness, porosity and cortical thickness. Such complex manifestations of osteoporosis require the evaluation of multiple parameters with different sensitivities to the various properties of bone that are affected by the disease. This objective may be achieved by using a multi-frequency ultrasonic examination. The ratio of the acoustic wavelength to the cortical thickness can be changed by varying the frequency of the ultrasonic pulse propagating through the long bone that results in the change in composition of the induced wave comprised of a set of numerous modes of guided, longitudinal, and surface acoustic waves. The multi-frequency axial transmission QUS method developed at Artann Laboratories (Trenton, NJ) is implemented in the Bone Ultrasonic Scanner (BUSS). In the current version of the BUSS, a train of ultrasonic pulses with 60, 100, 400, 800, and 1200 kHz frequencies is used. The developed technology was tested on a variety of bone phantoms simulating normal, osteopenic, and osteoporotic bones. The results of this study confirm the feasibility of the multi-frequency approach for the assessment of the processes leading to osteoporosis.

Keywords

Bone quantitative ultrasound; multi-frequency axial transmission scanner; osteoporosis

Introduction

The diagnosis of osteoporosis has been improved by the development of new quantitative methods of skeletal assessment; however, the advanced methods like quantitative computed tomography are technically challenging and not widely accepted [1]. Thus, the development of a portable and affordable technique for the assessment of bone quality in osteoporosis with improved ability for prediction of fracture risk, monitoring of treatments, and

© 2013 Elsevier B.V. All rights reserved.

Corresponding author: Alexey Tatarinov 1459 Lower Ferry Rd, Trenton, NJ 08618, USA alta2003@apollo.lv Tel: (609) 883-0100 Fax: (609) 858-5233.

Publisher's Disclaimer: This is a PDF file of an unedited manuscript that has been accepted for publication. As a service to our customers we are providing this early version of the manuscript. The manuscript will undergo copyediting, typesetting, and review of the resulting proof before it is published in its final citable form. Please note that during the production process errors may be discovered which could affect the content, and all legal disclaimers that apply to the journal pertain.

identifying the populations at risk is important. Low bone material density (BMD) as diagnosed by dual-energy x-ray absorption (DXA) is only one of the contributing factors to skeletal fragility [2]. Fracture risk is also increased by the reduction of bone mass, and by the micro-architectural deterioration of the bone tissue [3]. Bone ultrasonometry, or quantitative ultrasound (QUS), is a simple, safe, and cost-effective technique that is sensitive to the mechanical and structural features of the bone, and has potential to become an effective complement or alternative to DXA [4, 5]. Only heel QUS devices are currently acknowledged as decision making tools for osteoporosis [6]. These devices apply through-transmission ultrasound to the spongy bone of the calcaneus and measure the ultrasound velocity or “speed-of-sound” (SOS) as well as the broadband ultrasound attenuation (BUA).

Axial transmission ultrasonometers, or axial transmission QUS devices, work with the compact tissue of the accessible long bones, such as the tibia and the radius [7]. The probes are placed along the body part over the examined bone and radiate ultrasound waves into the cortical layer through the surface layer of soft tissues. Commercial axial transmission ultrasonometers typically measure the ultrasound velocity at fixed frequencies close to 1 MHz [8, 9]. This velocity corresponds to the propagation of longitudinal ultrasonic waves. It varies from 3.5 to 4.2 km/s and is mainly sensitive to the variations in the elastic modulus of the compact bone. The longitudinal waves mostly propagate in the surface layer of the cortex, near the periosteum, and their propagation velocities are weakly sensitive to the progression of porosity away from the endosteum. The uncertainty of these measurements is increased by the variations of the mineralization degree and the intracortical porosity. This limitation has led to the criticism that axial transmission ultrasonometers have a low specificity to osteoporosis manifestations and a weak sensitivity to the disease's incipience [10, 11].

Novel approaches to the evaluation of cortical bones with respect to osteoporosis have been explored in recent years. One of these approaches applies through-transmission ultrasound directly to the diagnostically important sites, the hip and the forearm, that are composed mainly of cortical bone. A scanner for the femoral neck has also been developed [12]. It depicts the bone inside the body and measures the SOS and the BUA in a way similar to the heel QUS. Another device has been proposed and constructed to evaluate the ultrasound propagation through the arm radius bone at a single location by through-transmission [13]. The device is based on an array of 64 transducers and measures the SOS in the bone by calculating the difference in the transmit times between ultrasonic pulses propagating through the bone and the soft tissues, and the ultrasonic pulses propagating through the soft tissues alone. A promising approach based on ultrasonic backscattering from the cortical sites has also been proposed [14]. The values of the integral backscatter in the radius and the tibia correlate with the BMD in the femoral neck.

Axial transmission QUS using surface transmission of ultrasonic waves has the advantages of easy unilateral access to the measurement sites and the compactness of the ultrasonic hardware. Dzenis et al. first performed a detailed investigation of the topographical patterns of ultrasound velocity in long bones at low frequencies (around 100 kHz) using point-contact transducers on a short acoustic base in the 1980s [15, 16]. They used an ultrasonic system originally developed for non-destructive testing of construction materials. The

topographical variation of acoustic properties of long bones, particularly the velocity of slowly propagating flexural waves, was shown to be highly sensitive to the conditions of the bones [17-19].

The last decade has seen a major surge in the development of axial transmission QUS technologies based on the use of guided acoustic waves having the wavelengths close to or exceeding the cortical thickness [20-27]. Numerical modeling techniques and physical models have been used to study propagation of the various modes of acoustic waves in bones under different boundary conditions. The relationships between the velocities of various acoustic wave propagation modes and the elastic properties of the bone as well as the cortical thickness have been investigated. The phase and group velocities of guided waves have a characteristic nonlinear dependence on the ratio of the bone thickness to the ultrasonic wavelength, a phenomenon known as geometrical dispersion [28]. The velocities of guided waves have been demonstrated to be considerably more sensitive to the manifestations of osteoporosis than the velocities of longitudinal waves [20, 29]. The high correlation of guided wave velocities to the cortical thickness (CTh) has been shown for the distal radius *in vitro*. The velocity was determined for the intensity maxima of the received signals using different methods of processing, such as singular value decomposition [30] and two-dimensional spectral analysis based on group velocity filtering and the fast Fourier transform [23].

The condition of cortical bones is determined by numerous mechanical, micro-structural, and geometrical or macro-structural properties like hardness, porosity, and cortical thickness. There are significant limitations to osteoporosis assessment when only one frequency is used to probe a single anatomical location. The complex manifestations of osteoporosis require the evaluation of multiple ultrasonic parameters with different sensitivities to the various properties of bone that are affected by the disease. Aged bones may demonstrate little or no decrease in mineralization [31] which is the main feature affecting the SOS, a key measurable of conventional QUS. Aged bones may also demonstrate hypermineralized areas [32], adding a confounding factor to increased porosity and thus reducing the efficiency of osteoporosis detection by conventional axial transmission QUS.

The main hypothesis of the presented study is that complex nature of the processes leading to osteoporosis requires a multi-frequency ultrasonic examination, which has a potential of differential sensitivities to the various bone properties affected by aging and disease. The ratio of the acoustic wavelength to the cortical thickness can be changed by varying the frequency of the ultrasonic pulse propagating through the long bone. As a result, the composition of the propagating wave packet comprised of various acoustic wave modes changes. This change is the basis for using a multi-parameter classifier in further clinical studies [33].

Design and function of the multi-frequency Bone UltraSonic Scanner (BUSS)

The multi-frequency axial transmission QUS method developed at Artann Laboratories is implemented in the Bone Ultrasonic Scanner (BUSS). The BUSS consists of the two major components: a hand-held ultrasonic probe and a portable electronics unit. The electronics

unit includes a computer with an integrated ultrasonic data acquisition board. The device has a small footprint and may be placed on the physician's table or a movable cart. A general view and block diagram of the BUSS are depicted in Fig.1.

The data acquisition board is based on the EP2C5Q208C7 field-programmable gate array (FPGA) from the Altera Corporation Cyclone®II family. It executes pre-loaded command sequences, sets the output amplification, synchronizes the output and input data frames, receives the digitized ultrasonic signals, records the signals to a buffer memory for transmission to the computer, and performs preliminary processing, such as averaging. The computer first loads the commands and data necessary to transmit the correct ultrasonic waveforms to the RAM-1 storage. The FPGA is then ready to execute these commands to generate the output signals. The structure of the output signals is defined by the recorded 12-bit data frames which are read cyclically from RAM-1.

The excitation waveforms are short pulses with two sinusoidal periods under a Gaussian function envelope. A unique and proprietary feature of the BUSS is that each measurement is conducted by transmitting a train of these short ultrasonic pulses with different carrier frequencies. The current version of BUSS transmits a train of 5 pulses with the following carrier frequencies: 60 kHz, 100 kHz, 400 kHz, 800 kHz, and 1200 kHz. The output voltage of the transmitter is 150 V peak-to-peak. The entire transmitted frame is comprised of 32,000 samples with a 33 MHz sampling rate.

The transmitted acoustic signal is captured by the receiver and digitized using a high-speed analog-to-digital converter. The analog signals are conditioned by a voltage-gain preamplifier and a low-pass filter with cutoff frequency 2.5 MHz at -5dB and slope -20 dB/decade. The FPGA records the digitized signals to RAM-2. Multiple sets of data trains are recorded and averaged within the FPGA before they are transferred to the computer via USB. The acquired data frame is of the same size as the transmitted waveform data frame.

The computer guides the user through the measurements using a graphical user interface, performs data analysis and displays the exam output. The current BUSS uses a Dell Inspiron Mini Netbook embedded in a unified enclosure with the ultrasonic acquisition board (Fig.1). The 1.6 GHz processor with a 400 MHz 1 MB cache, 400 MHz 1GB RAM, 20 GB hard drive, and USB 2.0 computer handles the computations. The software allows the user to input various subject and examination metadata. It records 15 sequential ultrasonic measurements along the subject's proximal tibia and acquires the ultrasonic propagation signals at 5 different frequencies for each measurement. The software provides real-time feedback to the operator about the quality of the acoustic contact based on various received signal parameters, and guides the operator with the system messages.

The ultrasonic data processing involves analysis of a set of 75 acquired signals (15 points × 5 frequencies) to calculate a set of parameters for the various modes of acoustic wave propagation. The area of the proximal tibia that is examined by the BUSS features a varied content of cortical and underlying trabecular bone tissues with a continuous natural gradient of the cortical thickness from the bone epiphysis to the diaphysis. An applicator is placed on the front of the subject's tibia, in the region of the tibia medial surface, to facilitate the

correct scanning procedure. The applicator is a disposable, 40 micron thick, acoustically transparent film made of a medical grade polymer. It has markings indicating the correct placement of the probe for each of the 15 measurement points at 10 mm intervals. E-Z Lubricating Jelly from Chester Labs, Inc. is used to lubricate the applicator and provide ultrasonic coupling.

The BUSS broadband probe

The BUSS probe (Fig.2) provides an ergonomic handgrip that allows an operator to comfortably take the required multiple measurements along the subject's bone. It acquires ultrasound signals that propagate through the tibia by surface transmission from the emitter to the receiver. The probe is positioned in the medial surface of the tibia, wherein the transducers' base is oriented along the longitudinal axis of the bone. Typically, the contact pressure is within the range of 2-3N. Its adequacy is verified by the 100 kHz signal amplitude, which has a threshold at the pre-set level. The probe includes a pair of ultrasonic transducers and a preamplifier for the received ultrasonic signals. The design ensures acoustic isolation between the transducers, preventing ultrasonic signals from propagating directly from one to the other through the probe body. The rigidity and close fit of the transducer seats in the probe handle ensures stable ultrasonic measurements. The acoustic base is fixed at 40 ± 0.1 mm.

The preamplifier is a small printed circuit board with an Analog Device, Inc. AD8655ARZ low-noise precision CMOS amplifier. The amplification coefficient is set to 10. The board is mounted within the probe handle. All of the probe components may be easily removed for repairs or replacement.

The bandwidth of the transducers used in the BUSS probe was a key point in the design. The multi-frequency measurements required a full order of magnitude range from less than 0.1 MHz to 1.0 MHz. The broadband transducer design (Fig.2) is based on a miniature piezoelectric PZT prism with no sharp resonances in the working frequency band. Both the emitting and the receiving elements are 1 mm thick, 0.9 mm wide and 8.5 mm long. The piezoelectric material is a PI (Physik Instrumente), Ltd. PIC255 lead zirconate titanate PZT. Electrodes are connected to the metalized surfaces of the elements on both sides across their thickness using electrically conductive epoxy. The electrode on the outer side of the element is a thin metal wire that connects to the device's ground through a metal housing of the transducer. The hot electrode on the inner side of the element is a $\varnothing 1.5$ mm brass rod. The transducers are covered with a 0.5 mm layer of insulating epoxy resin. The piezoelectric element is embedded in a plastic material which serves as both the matching waveguide and the acoustical backing that dampens the transducer, reducing the number of periods in the emitted pulse to one period with the highest amplitude. The criteria for the transducers' bandwidth acceptability were the ability to generate relatively short (one to two periods) pulses at the selected frequencies within the 60-1200 kHz band, and the coincidence of the central frequency of the emitted pulse to the central frequency of the excitation waveform. The output signals from emitters were recorded through air from the transducer's tip by a laser vibrometer and in a water tank by a pair of symmetric transducers using through-

transmission from a distance of a few centimeters. The spectra were calculated using the fast Fourier transform of the received signals.

Multi-frequency operation of the BUSS

The main innovation implemented in the BUSS is the use of the multi-frequency mode for bone assessment. It is necessary to make measurements at a larger set of frequencies to separate the contribution of the different modes of the acoustic waves in the received signals and to evaluate their propagation parameters.

Fig.3 illustrates the approach implemented in the BUSS. Each measurement along the bone is conducted using a train of short ultrasonic pulses with different carrier frequencies. The BUSS was initially programmed to send and receive a train of 10 pulses in the 0.1-1.2 MHz range band with the following carrier frequencies: 0.1, 0.2, 0.3, 0.4, 05, 06, 07, 0.8, 1.0, 1.2 MHz (Fig.3 top two panels). The pulses were separated by the minimum time intervals that allow for separate acquisition of each pulse at the receiving transducer. Two bottom panels show examples of individual pulses in the transmitted (left column) and received (right column) signal trains at the selected frequencies.

Different types of received acoustic waves (shown in the right column of Fig.3) become apparent at different frequencies and can be identified as bulk waves (the fastest wave component at high frequencies), surface waves (the slower wave component of greater amplitude at high frequencies), and guided waves at low frequencies.

In its geometry, cortical bone is represented by a shell of complex shape, a fragment of which can be roughly approximated by a plate or a fragment of a tube. The ratio of the cortical thickness to the ultrasonic wavelength is changed by varying the ultrasonic frequency over a wide range. The larger the ratio of the wavelength to the cortical thickness, the closer the propagation of the acoustic wave is to that in a thin plate. The smaller the ratio, the closer the wave propagation is to that in the half-space, namely the surface waves. The most comprehensive analysis of plate waves and surface waves is presented in [28]. At the lower frequencies, where ultrasonic wavelength is much larger than the cortical thickness, the bone behaves like a thin plate. In thin plates the acoustic energy propagates in the form of the various modes of guided waves, such as symmetric and antisymmetric Lamb waves. The zero-order antisymmetric Lamb wave, also called flexural wave, is a slow-type wave with a non-linear dependence of the wave velocity on the plate thickness. The flexural wave dominates in amplitude over the first coming symmetric Lamb wave and can thus be identified in the wave packet. Increasing the thickness-to-wavelength ratio transforms the Lamb wave into a surface Rayleigh wave on the plate surface. In contrast to the flexural wave the velocity of the surface Rayleigh wave is not dependent on the thickness. The longitudinal wave and the surface wave are detected together.

The relatively large (two- to three-fold) variations in the cortical thickness between individuals and along the bone length in a single individual are the most significant factors influencing the flexural wave propagation at low frequencies (60-100 kHz). The material properties of bone tissue, such as the elastic constants affected mostly by tissue mineralization, vary with aging to a much lesser degree, not exceeding 10-15% [34]. To

reduce the influence of the geometrical factor, the inner material properties affected by the tissue composition (degree of the mineralization) and the defects of the microstructure (microcracks, intracortical porosity), are assessed by ultrasonic measurements at higher frequencies, from several hundred kilohertz to one megahertz. Our model studies [35] showed that by increasing ultrasonic frequency to 500 kHz, the longitudinal wave velocity measured by the first arrival at the axial transmission mode is sensitive to the changes within the surface layer not exceeding 2 mm. Thus, the measurements at the high frequency are sensitive to the growth of intracortical porosity in the metaphyseal areas of the bones, where the cortex is thin. The medium frequencies (200-400 kHz) also carry useful information because they represent an intermediate condition, where influence of the cortical thickness is not as expressed as it is at the low frequencies. However, the wavelength at these medium frequencies is large enough to capture features of the deeper layers of the cortex. The interference of the mixed modes at medium frequencies can form specific patterns of spatio-temporal waveform profiles along bones, characterizing certain conditions in the bone. The data on the relationship between ultrasound propagation parameters at different frequencies and the conditions of bone *in vivo* are presented in the companion paper in this issue [33].

We estimated that five ultrasonic pulses in the transmitted train would be sufficient to provide the structural information about the bone conditions. The additional information that may result from increasing the number of pulses with different frequencies is negligible. Thus, to avoid unnecessary complexity in the system, the current version of the BUSS uses a train of five ultrasonic pulses at the 60, 100, 400, 800, and 1200 kHz frequencies.

Bench testing of BUSS

The BUSS bench testing on models was intended to demonstrate the feasibility and effectiveness of the multi-frequency principle for the assessment of the cortical bones in osteoporosis. Bone resorption in osteoporosis starts from the endosteal surface, bordering the medullar cavity, and eventually leads to the thinning of the cortex and the trabecularization of the inner cortical layer. Demineralization and hypermineralization of the bone affect the mechanical properties and consequently the ultrasound velocity in the outer layer of the bone. Inner porosity in the cortical bone layer also affects its effective elastic modulus. The thinning of the cortex is one of the main indicators of a lower overall bone strength and a diminished capacity to withstand fracturing. The development of intracortical porosity is another factor in determining the degradation of the bone quality and the risk of brittle fracturing.

A variety of bone phantoms have been made to simulate normal, osteopenic, and osteoporotic bones (Fig.4): (a) phantoms consisting of layers of different thickness of a hard epoxy (mimicking cortical bone) and an epoxy layer filled with small soft rubber particles (0.5 to 1 mm, mimicking porous bone); and (b) phantoms manufactured using a 3-D printer with a designed thickness and pore distribution, in which the voids mimicking the pores were programmed as 1 mm spheres filled by the soft support material used in the 3-D printing process. The resolution of the 3-D printer is 40 microns. The Stratasys Objet 3D printer was used to create these models. The bone structure was modeled using the rigid

VeroGray RGD850 material, while the pores filled with a soft substance were modeled by the wax-like support material.

Fig.5 illustrates changes in the signals within a multi-frequency train at a single point on bone-mimicking phantoms. The 3 mm thick hard epoxy plates with different pore content as shown on the left panel of Fig. 5 were tested. The first specimen simulated healthy bone and contained no pores; the second specimen had 30% pores by volume at the bottom layer (approximately half of its thickness); the third specimen contained 30% pores by volume distributed throughout its entire bulk. A dramatic attenuation of high frequency signals is observed as the porosity increases.

The BUSS is designed to make scanning measurements along the tibia from the epiphyses towards diaphysis covering a distance of 15 cm, where the cortical thickness varies from one to several millimeters. A set of phantoms with a wedge-shaped cross section and linear thickness gradient were designed and manufactured on the 3-D printer to mimic this feature. The phantoms had a 15 cm long testing area and were 18 mm wide. Three bone conditions were modeled: “healthy”, “osteopenic”, and “osteoporotic”. In the “healthy” phantom, the thickness varied from 3 mm at the thin end to 9 mm at the thick end. “Osteopenia” and “osteoporosis” phantoms had the thickness variation from 1 to 6 mm. “Osteoporosis” phantom had a layer of pores at the bottom. The measurement procedure illustrated in Fig.6 mimicked the clinical examination: data were acquired in 15 zones along the phantom. Fig.7 shows the recorded ultrasonic profiles at the four selected frequencies: 60 kHz, 100 kHz, 400 kHz and 1200 kHz, i.e. the low, middle, and high frequencies in the BUSS band. One can follow specific trends from “norm” to “osteoporosis” through “osteopenia” in each column of the spatio-temporal waveform profiles related to the chosen low, middle, and high frequencies. Although the trends are consistent at all frequencies, their features and manifestations are different. At 60 kHz and 100 kHz the most notable aspects are the shift of the slow wave component intensity maxima and the increase of the profile's gradient from “norm” to “osteoporosis”. This is a result of the so called “geometrical dispersion” – the dependence of the zero-order antisymmetric Lamb wave velocity in thin plates on the thickness of the plate [28]. The thickness-to-wavelength ratio is lower at 60 kHz than at 100 kHz, thus the flexural wave velocity is lower and the propagation time is longer at 60 kHz at the same measurement location along the phantom. In accordance with the thickness gradient along the phantom, the corresponding gradient of the spatio-temporal waveform profile at 60 kHz is steeper than at 100 kHz. The difference between the profile graphs at 60 kHz and 100 kHz is expressed more in the “osteoporotic” phantom, where the solid layer is thinner. The difference is most expressed at the thin ends of the phantoms modeling the bone metaphysis. It follows that even a moderate (several tens of kilohertz) variation of frequency in the lower frequency range can cause a notable change in the waveform profiles for guided waves. This effect can be used as a diagnostic approach to reveal the changes in the cortical thickness along the bone length.

Some of the ultrasound propagation parameters obtained at different frequencies are directly related to the quantitative characteristics of the bone that are relevant for osteoporosis diagnostics. This was shown in our earlier experiments on long bones *in vitro* [36, 37]. Fragments of human proximal tibiae were examined using the dual-frequency BUSS

prototype and peripheral quantitative computed tomography (pQCT). The samples varied in the volumetric bone mineral density (BMD) and the cortical thickness (CTh) within the typical range from upper norm to expressed osteoporosis. These parameters correlated with each other since both of them are affected by osteoporosis. Fig.8 presents some of the data obtained in that study showing that the ultrasonic data obtained at different frequencies allows the direct assessment of the diagnostically relevant characteristics of the bone. Fig. 8A shows a linear correlation between the observed cortical BMD and the longitudinal wave velocity measured at 400 kHz with the Pearson linear correlation coefficient of 0.93. A good correlation with the CTh was obtained for the guided wave velocity at 100 kHz (Fig.8B) using arrival time of the slow wave component distinguished by its higher amplitude in the received wave packet. The dependence has characteristics similar to that of the zero-order antisymmetric Lamb wave (or flexural wave). The specific non-linear character of the dependence was analyzed in more detail in our earlier publication [36]. The Spearman rank correlation coefficient for this dependence was found to be 0.83. A discrepancy between the CTh measured by pQCT and the effective CTh that is determined by the velocity of the guided wave is illustrated in Fig.8C. It is caused by the increased porosity in the endosteal layer of the cortex and the absence of a precise boundary between the trabecular and cortical components. The estimation of the CTh in cases of blurred boundaries is highly dependent on the pQCT detection thresholds. In fact, the effective CTh in several areas that involve the proper cortical component and the unaccounted part of the adjacent trabecular bone can be larger than that estimated by pQCT. Therefore the measured velocity values of the flexural wave in these areas are higher than those expected from the CTh data provided by pQCT (Fig.8B).

The waveform profiles for 1200 kHz shown in the right column of Fig.7 demonstrate the most drastic difference between the “osteoporosis” case and the “norm” and “osteopenia” cases. The completely blank area with no detectable signals in the “osteoporotic” phantom indicates increased attenuation due to the scattering by the simulated pores, similar to that demonstrated above in Fig.5. This temporal area of damped signals corresponds to the places where the fast propagating longitudinal wave arrives in the case of *in vivo* measurement. The signal damping in this area may be indicative for porosity. At the middle frequency of 400 kHz, where the mixed acoustic wave modes are present, the waveform patterns, such as those illustrated in Fig.7, are difficult to interpret. However, the overall views of the spatio-temporal waveform profiles in the three phantoms shown in Fig.7 are different and the waveform profiles can be analyzed as abstract images sensitive to bone conditions. The potential sensitivity of multi-frequency axial transmission scanning ultrasonometry to the conditions of the long bone shown in the phantom studies was also confirmed in clinical studies on 331 subjects described in detail in the companion paper included in this special issue of Ultrasonics [33]. In the study described in that paper, the efficiency of the BUSS for osteoporosis detection was assessed using a receiver operating characteristic curve analysis. A linear classifier was derived which provided at its output 87.7% sensitivity and 63.2% specificity to DXA-identified osteoporosis. The parameters used in the classifier included: the amplitudes of the received waves at different frequencies or their ratios, the waveform profiles along the tibia at different frequencies or affinity

indexes, the wave propagation speed or signal position in time, and the shift of the wave pulse center frequency.

Conclusion

The results of this study confirm the feasibility of the multi-frequency approach for the assessment of the processes leading to osteoporosis. The multi-frequency approach allows one to derive a plurality of ultrasonic parameters with differential sensitivity to the various bone properties affected by aging and disease from the ultrasound axial transmission data obtained in a wide range of frequencies from 60 to 1200 kHz.

Acknowledgments

The authors gratefully acknowledge Aleksandr Pasechnik for his contribution in the review and editing of the manuscript. The research reported in this publication was supported by the National Institute on Aging of the National Institutes of Health under Award Number R44AG017400. The content is solely the responsibility of the authors and does not necessarily represent the official views of the National Institutes of Health.

References

1. Adams JE. Advances in bone imaging for osteoporosis. *Nat. Rev. Endocrinol.* 2013; 9(1):28–42. [PubMed: 23232496]
2. Baim S, Leslie WD. Assessment of fracture risk. *Curr. Osteoporos. Rep.* 2012; 10(1):28–41. [PubMed: 22274642]
3. Bouxsein ML, Seeman E. Quantifying the material and structural determinants of bone strength. *Best Pract. Res. Clin. Rheumatol.* 2009; 23(6):741–53. [PubMed: 19945686]
4. Laugier P. Instrumentation for in vivo ultrasonic characterization of bone strength. *IEEE Trans. Ultrason. Ferroelectr. Freq. Control.* 2008; 55(6):1179–1196. [PubMed: 18599407]
5. Gregg EW, Kriska AM, Salamone LM. The epidemiology of quantitative ultrasound: a review of the relationships with bone mass, osteoporosis and fracture risk. *Osteopor. Int.* 1997; 7:89–99.
6. Krieg MA, Barkmann R, Gonnelli S, Stewart A, Bauer DC, Del Rio Barquero L, Kaufman JJ, Lorenc R, Miller PD, Olszynski WP, Poiana C, Schott AM, Lewiecki EM, Hans D. Quantitative ultrasound in the management of osteoporosis: the ISCD official positions. *J. Clin. Densitom.* 2008; 11:163–187. 2007. [PubMed: 18442758]
7. Hans, D.; Bo, F.; Fuerst, T. Non-heel quantitative ultrasound devices. In: NJeh, CF.; Hans, D.; Fuerst, T.; Gluer, CC.; Genant, HK., editors. *QuantitativeUltrasound: Assessment of Osteoporosis and Bone Status*. Martin Dunitz; London: 1999. p. 145-162.
8. Njeh CF, Saeed I, Grigorian M, Kendler DL, Fan B, Shepherd J, McClung M, Drake WM, Genant HK. Assessment of bone status using speed of sound at multiple anatomical sites. *Ultrasound Med. Biol.* 2001; 27(10):1337–1345. [PubMed: 11731047]
9. Prevrhal S, Fuerst T, Fan B, Njeh C, Hans D, Uffmann M, Srivastav S, Genant HK. Quantitative ultrasound of the tibia depends on both cortical density and thickness. *Osteoporos. Int.* 2001; 12(1): 28–34. [PubMed: 11305080]
10. Christian R, Krestan CR, Grampp S, Henk C, Peloschek P, Imhof H. Limited diagnostic agreement of quantitative sonography of the radius and phalanges with dual-energy X-ray absorptiometry of the spine, femur, and radius for diagnosis of osteoporosis. *AJR.* 2004; 183:639–644. [PubMed: 15333350]
11. Tuna H, Birtane M, Ekuklu G, Cermik F, Tuna F, Kokino S. Does quantitative tibial ultrasound predict low bone mineral density defined by dual energy Xray absorptiometry? *Yonsei Med J.* 2008; 49:436–442. [PubMed: 18581594]
12. Barkmann R, Laugier P, Moser U, Dencks S, Klausner M, Padilla F, Haïat G, Glüer CC. A device for in vivo measurements of quantitative ultrasound variables at the human proximal femur. *IEEE Trans. Ultrason. Ferroelectr. Freq. Control.* 2008; 55(6):1197–204. [PubMed: 18599408]

13. Stein EM, Rosete F, Young P, Kamanda-Kosseh M, McMahon DJ, Luo G, Kaufman JJ, Shane E, Siffert RS. Clinical assessment of the 1/3 radius using a new desktop ultrasonic bone densitometer. *Ultrasound Med. Biol.* 2013; 39(3):388–395. [PubMed: 23312957]
14. Karjalainen J, Riekkinen O, Töyräs J, Kröger H, Jurvelin J. Ultrasonic assessment of cortical bone thickness in vitro and in vivo. *IEEE Trans. Ultrason. Ferroelectr. Freq. Control.* 2008; 55(10): 2191–2197. [PubMed: 18986867]
15. Dzenis VV, Purinsh YI. Ultrasonic flexural wave study of human skull bones. *Mechanics Composite Mat.* 1979; 15(3):297–301.
16. Dzenis VV. The Usage of Ultrasonic Transducers with Dry Point Contact for Non Destructive Testing, Zinatne, Riga. 1987 in Russian.
17. Dzene IY, Dzenis VV, Petuhova LI, Tatarinov AM, Yanson AY. Human tibia in the presence of coxarthrosis and fracture using exponential ultrasonic concentrators. *Mechanics Composite Mat.* 1980; 16(6):724–729.
18. Jansons H, Tatarinov A, Dzenis V, Kregers A. Constructional peculiarities of the human tibia defined by reference to ultrasound measurement data. *Biomaterials.* 1984; 5(4):221–6. [PubMed: 6487702]
19. Tatarinov AM, Dubonos SL, Yanson HA, Oganov VS, Dzenis VV, Rakhmanov AS. Ultrasonic diagnosis of the changes in human tibia during 370-day antiorthostatic hypokinesia. *Kosm. Biol. Aviakosm. Med.* 1990; 24(2):29–31. [PubMed: 2195232]
20. Nicholson PH, Moilanen P, Karkkainen T, Timonen J, Cheng S. Guided ultrasonic waves in long bones: modelling, experiment and in vivo application. *Physiol. Meas.* 2002; 23(4):755–776. [PubMed: 12450274]
21. Bossy E, Talmant M, Laugier P. Three-dimensional simulations of ultrasonic axial transmission velocity measurement on cortical bone models. *J. Acoust. Soc. Am.* 2004; 115:2314–2324. [PubMed: 15139643]
22. Muller M, Moilanen P, Bossy E, Nicholson P, Kilappa V, Timonen J, Talmant M, Cheng S, Laugier P. Comparison of three ultrasonic axial transmission methods for bone assessment. *Ultrasound Med. Biol.* 2005; 31(5):633–642. [PubMed: 15866413]
23. Moilanen P, Nicholson PH, Kilappa V, Cheng S, Timonen J. Assessment of the cortical bone thickness using ultrasonic guided waves: modelling and in vitro study. *Ultrasound Med. Biol.* 2007; 33(2):254–262. [PubMed: 17306696]
24. Moilanen P. Ultrasonic guided waves in bone. *IEEE Trans. Ultrason. Ferroelectr. Freq. Control.* 2008; 55:1277–1286. [PubMed: 18599415]
25. Protapappas VC, Fotiadis DI, Malizos KN. Guided ultrasound wave propagation in intact and healing long bones. *Ultrasound Med. Biol.* 2006; 32:693–708. [PubMed: 16677929]
26. Kilappa V, Xu K, Moilanen P, Heikkola E, Ta D, Timonen J. Assessment of the fundamental flexural guided wave in cortical bone by an ultrasonic axial-transmission array transducer. *Ultrasound Med. Biol.* 2013; 39(7):1223–1232. [PubMed: 23643059]
27. Xu K, Ta D, Wang W. Multiridge-based analysis for separating individual modes from multimodal guided wave signals in long bones. *IEEE Trans. Ultrason. Ferroelectr. Freq. Control.* 2010; 57(11): 2480–90. [PubMed: 21041135]
28. Viktorov, IA. Rayleigh and Lamb Waves: Physical Theory and Applications. Plenum Press; New York: 1967.
29. Sarvazyan A, Tatarinov A, Egorov V, Airapetian S, Kurtenok V, Gatt CJ Jr. Application of the dual-frequency ultrasonometer for osteoporosis detection. *Ultrasonics.* 2009; 49:331–337. [PubMed: 19036394]
30. Sasso M, Ha G, Talmant M, Laugier P, Naili S. Singular value decomposition based wave extraction in axial transmission: application to cortical bone ultrasonic characterization. *IEEE Trans. Ultrason. Ferroelectr. Freq. Control.* 2008; 55(6):1328–1332. [PubMed: 18599420]
31. Goldman HM, Bromage TG, Boyde A, Thomas CD, Clement JG. Intrapopulation variability in mineralization density at the human femoral mid-shaft. *J. Anat.* 2003; 203(2):243–255. [PubMed: 12924824]
32. Vajda EG, Bloebaum RD. Age-related hypermineralization in the female proximal human femur. *Anat. Rec.* 1999; 255(2):202–211. [PubMed: 10359521]

33. Egorov V, Tatarinov A, Sarvazyan N, Wood R, Magidenko L, Amin S, Khosla S, Ruhd R, Ruhd JM, Sarvazyan A. Osteoporosis detection in postmenopausal women using axial transmission scanning multi-frequency bone ultrasonometer: clinical results. *Ultrasonics*. (in print, this issue).
34. Malo MK, Rohrbach D, Isaksson H, Töyräs J, Jurvelin JS, Tamminen IS, Kröger H, Raum K. Longitudinal elastic properties and porosity of cortical bone tissue vary with age in human proximal femur. *Bone*. 2013; 53(2):451–458. [PubMed: 23334084]
35. Tatarinov A, Sarvazyan N, Sarvazyan A. Use of multiple acoustic wave modes for assessment of long bones: model study. *Ultrasonics*. 2005; 43(8):672–680. [PubMed: 15982472]
36. Tatarinov A, Sarvazyan A, Beller G, Felsenberg D. Comparative examination of human proximal tibiae in vitro by ultrasonic guided waves and pQCT. *Ultrasound Med. Biol.* 2011; 37(11):1791–1801. [PubMed: 21924819]
37. Tatarinov AM, Egorov VP, Sarvazyan AP. The dual-frequency method for ultrasonic assessment of skeletal system. *Acoust. Phys.* 2009; 55(4–5):665–673.

Highlights

- We describe a novel technology of multi-frequency axial transmission of cortical bones.
- Parameters of ultrasonic guided and bulk waves at different frequencies are differently sensitive to the cortical thickness and intracortical porosity.
- Structure and function of a new multi-frequency bone ultrasonometer are described.
- Bench testing in phantoms modeling thickness gradients and porosity in the cortex showed ability of the device to detect these changes.
- Waveform profiles along bones at different frequencies are specific to osteoporosis manifestations.

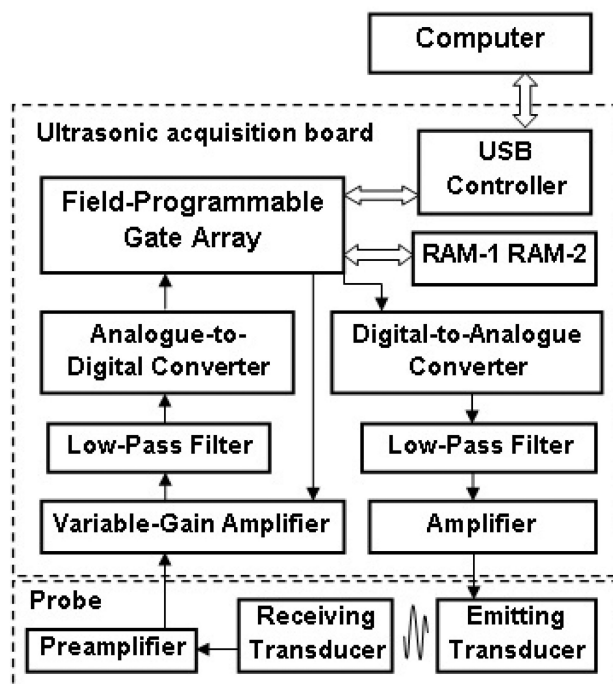
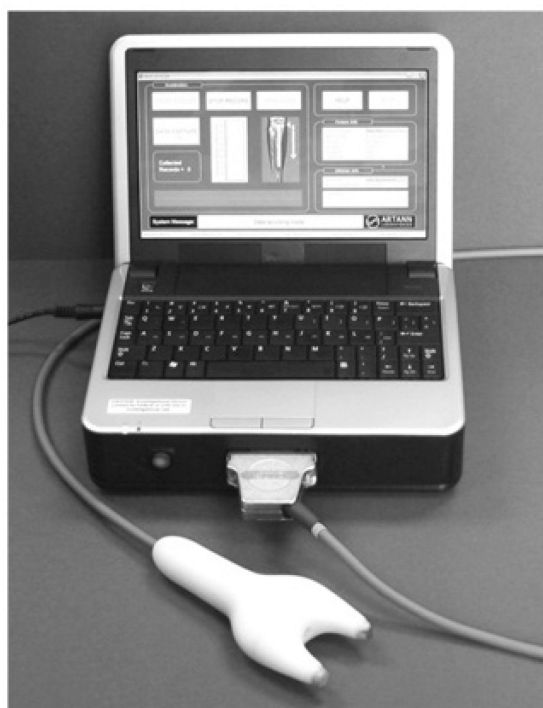


Fig.1.
General view and block-diagram of BUSS.

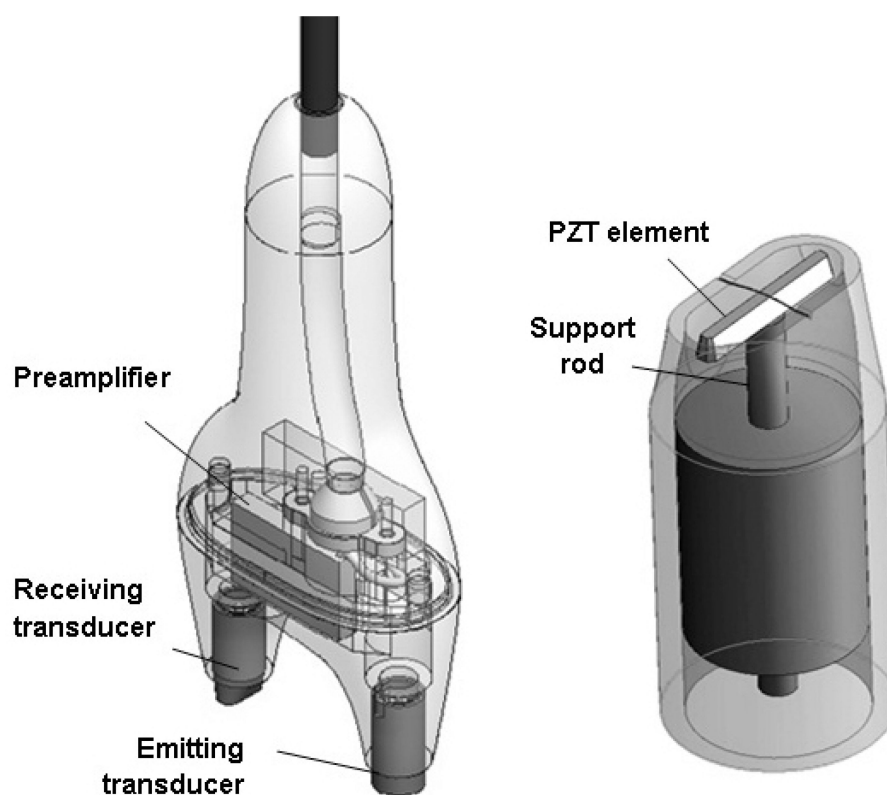


Fig.2.
Structure of BUSS probe and broadband transducer

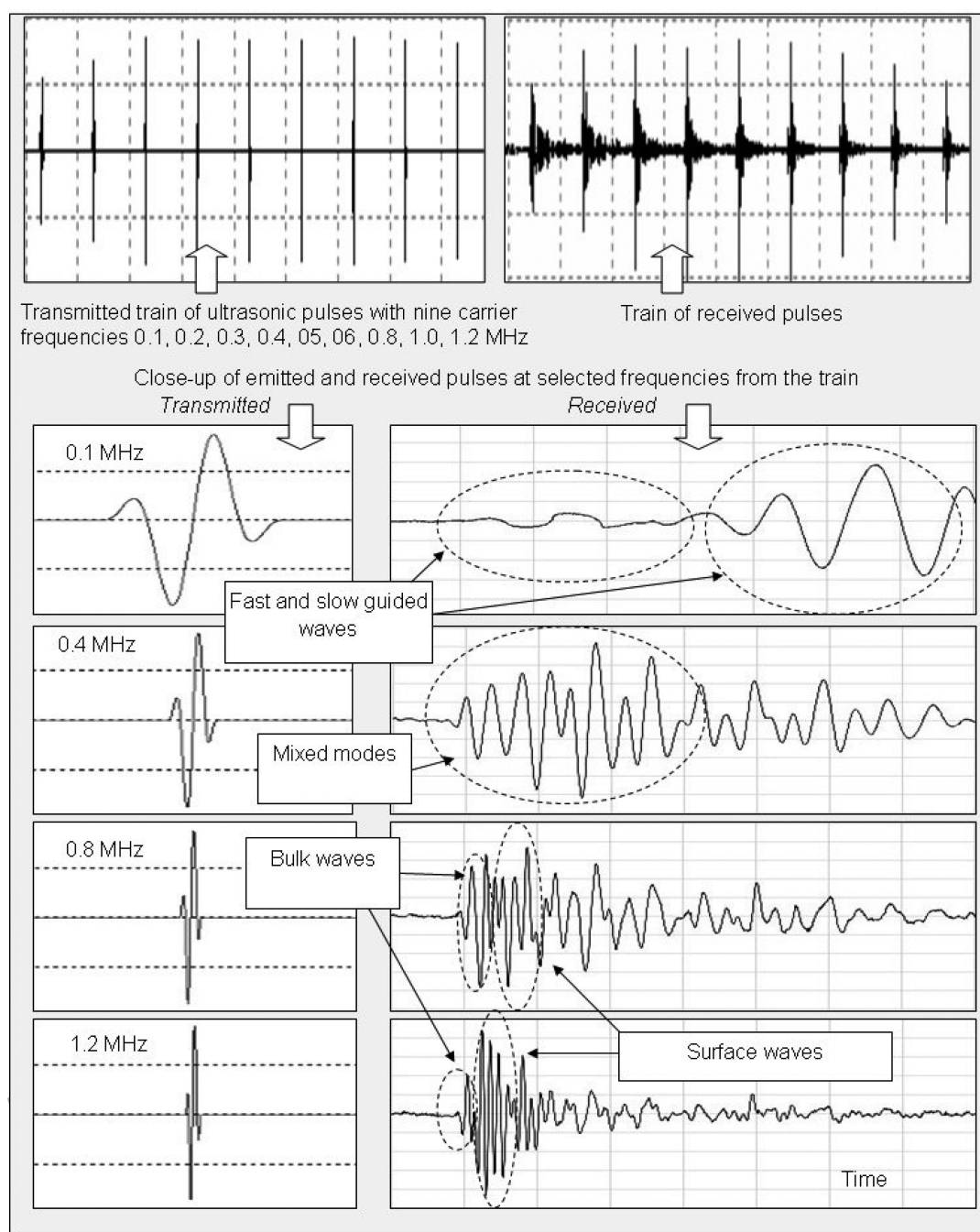


Fig.3.
Trains of transmitted and received ultrasonic pulses at multiple frequencies in the experiment on bone solid phantom.



Fig.4.
Examples of bone phantoms mimicking the normal, osteopenic and osteoporotic bones.

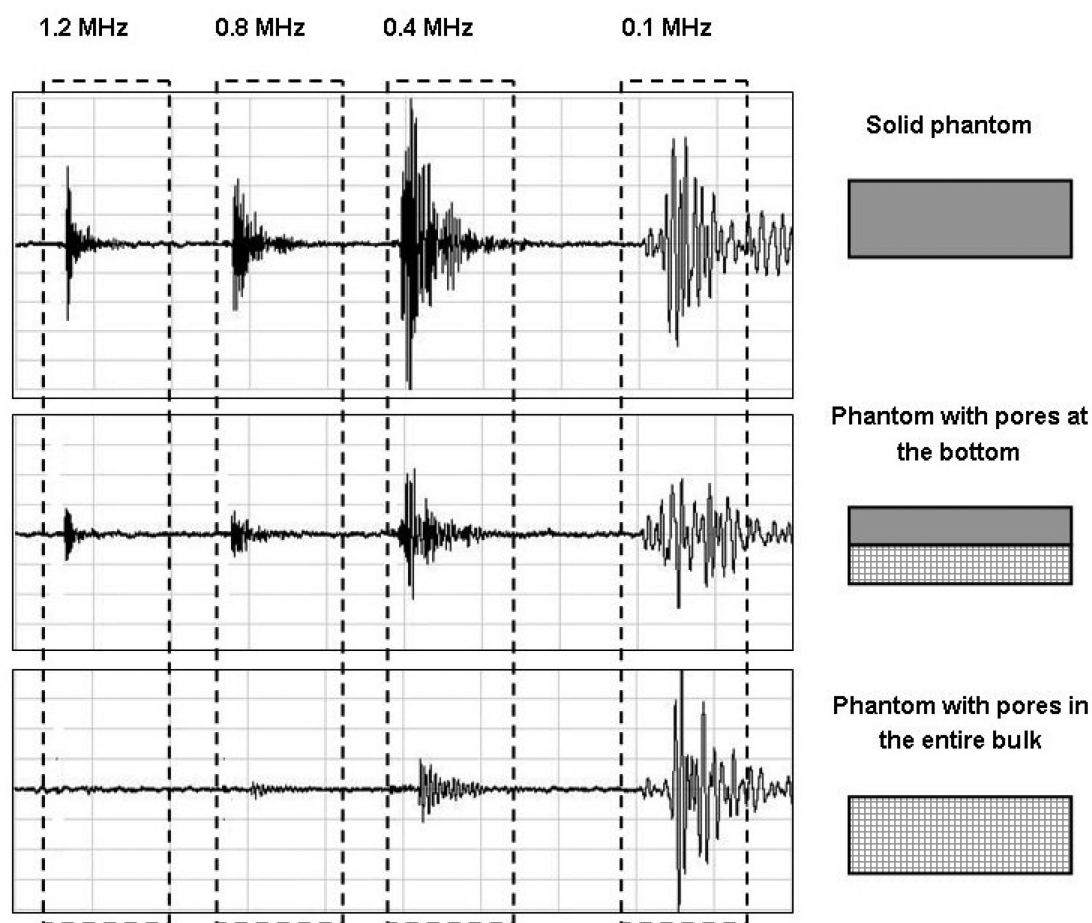


Fig.5.
Trains of received signals at frequencies 1.2, 0.8, 0.4 and 0.1 MHz in tree phantoms differing by the content of pores

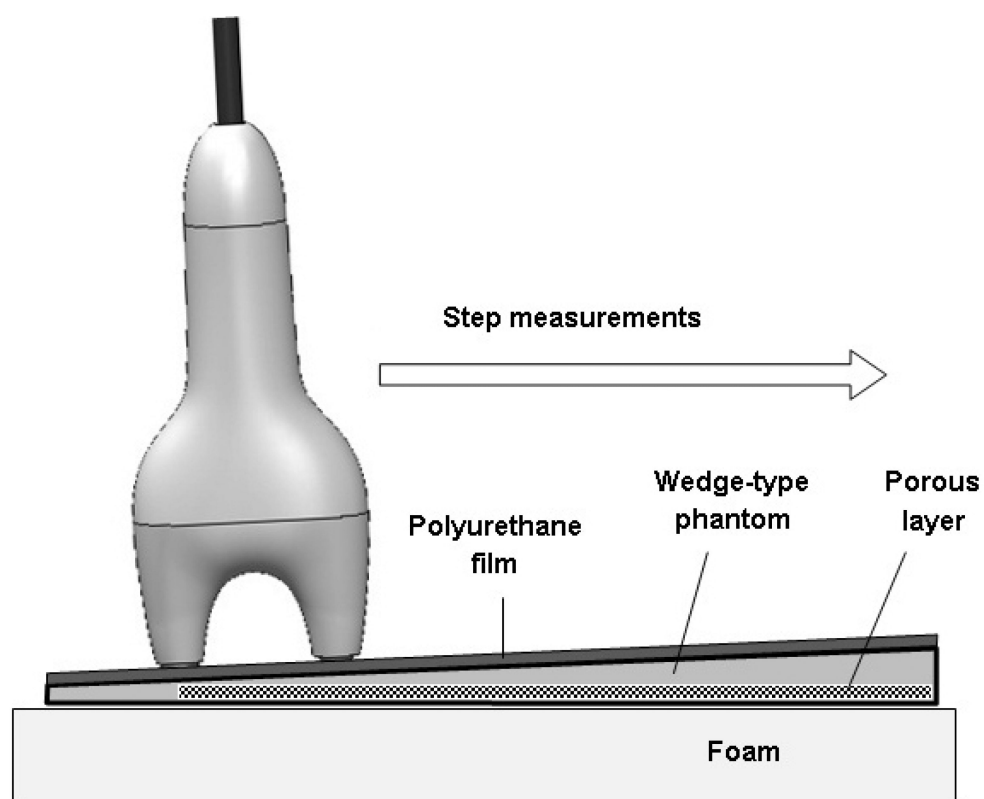


Fig.6.
Examination of bone wedge phantom. See text.

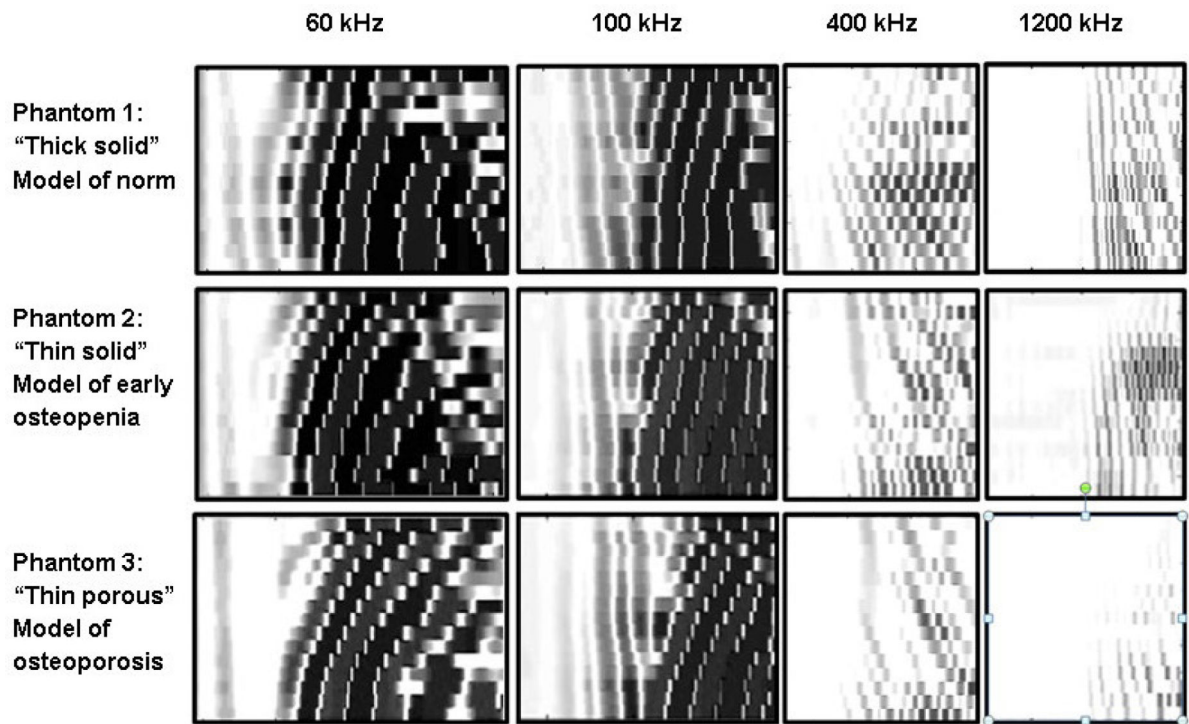


Fig.7.

Axial waveform profiles at 60, 100, 400 and 1200 kHz frequencies in three phantoms modeling conditions of norm, osteopenia and osteoporosis in cortical bones. Horizontal axis is ultrasound propagation time; vertical axis is phantom's length where each horizontal strip in profile corresponds to one measurement step of 1 cm.

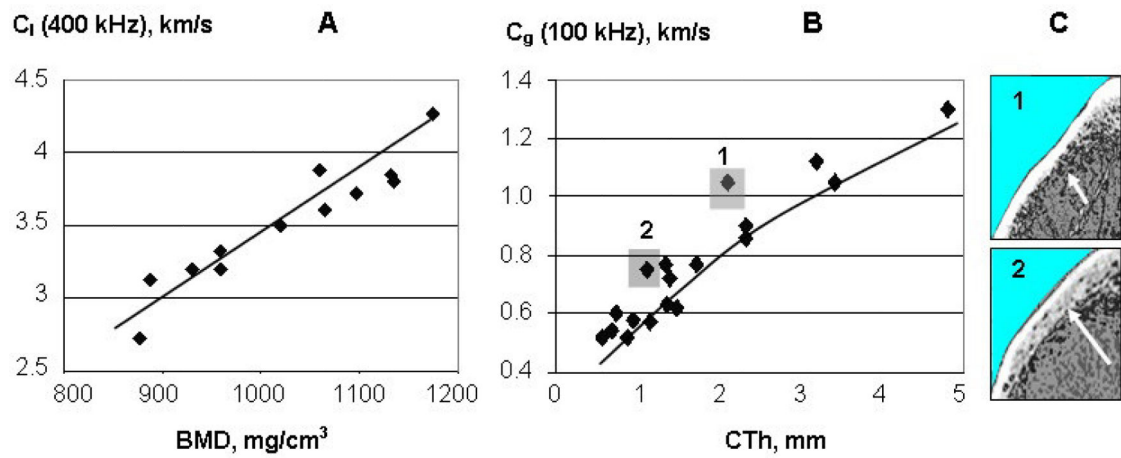


Fig.8.

Correlation graphs of velocity of longitudinal and guided waves with bone parameters in the experiment with *in vitro* bones [36]. A- longitudinal wave velocity C_l at 400 kHz vs cortical BMD; B – guided wave velocity C_g at 100 kHz vs cortical thickness CTh; C- illustrations of some discordance between cortical thickness estimated by pQCT and effective thickness of the cortical layer (see text)